APPENDIX

1. Calibration of methyl orange solutions

In order to determine the calibration curve of methyl orange solutions, the various concentrations of methyl orange solutions were prepared. The adsorbances of methyl orange solutions were measured using UV-VIS spectrophotometer at 465 nm.

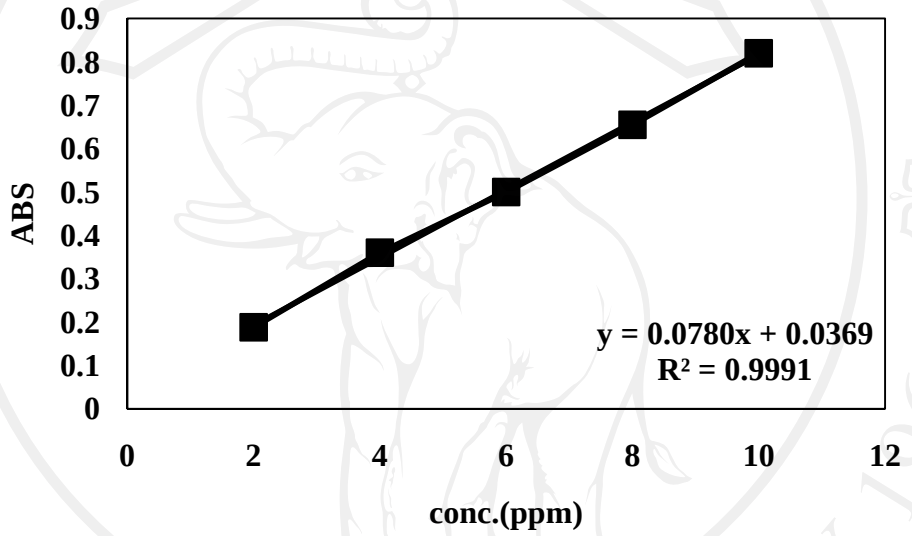

Figure. A Calibration curve of methyl orange solution.

Calculation of methyl orange concentration from calibration curve
Equation of calibration curve: $y = 0.0780x + 0.0369$
where y = absorbance and x = Calculation of methyl orange concentration

$$\text{Diluted methyl orange concentration} = \frac{\text{ABS} - 0.0369}{0.0780}$$

2. Calibration of iodine solutions

In order to determine the calibration curve of iodine solutions, the various concentrations of dihydrogenphosphate ion solutions were prepared. The absorbance of iodine was measured using UV-VIS spectrophotometer at 350 nm.

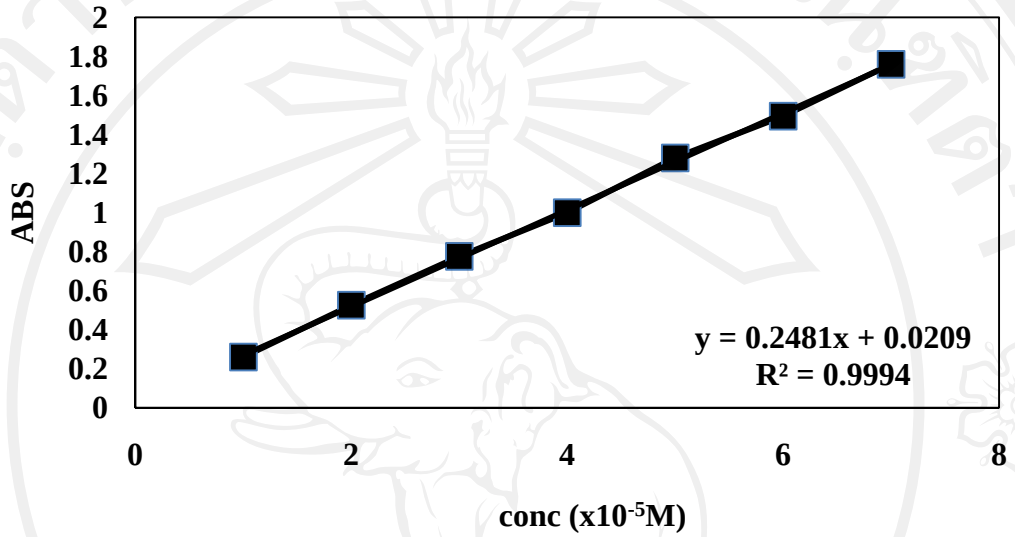

Figure. B Calibration curve of iodine solutions.

Calculation of iodine concentration from calibration curve
Equation of calibration curve: $y = 0.2481x + 0.0209$
where y = absorbance and x = Calculation of iodine concentration

$$\text{Diluted methyl orange concentration} = \frac{\text{ABS} - 0.0209}{0.2481}$$

2. **Scan of lambda max of methyl orange (10 ppm)**

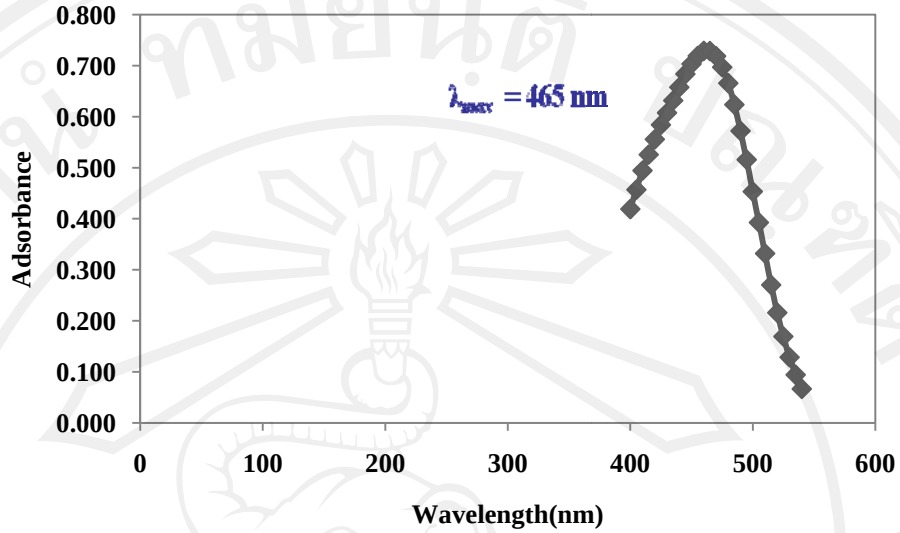

3. **Scan of lambda max of iodine ($1x10^{-5}$ M)**

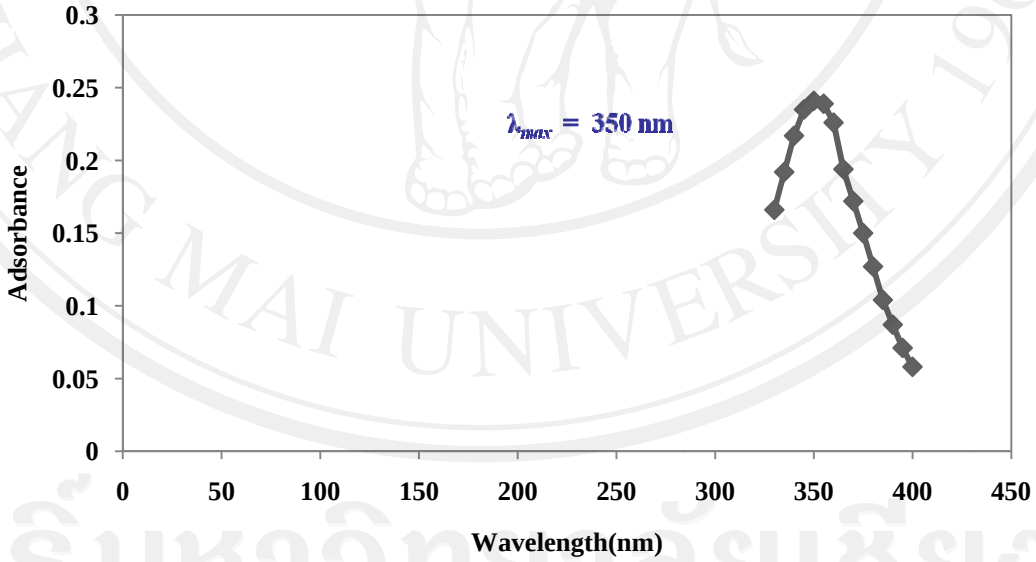

Table 4.5 Chemical composition of bottom ash, FGD gypsum and paddy soil by XRF.

Compound	Bottom ash	FGD gypsum	Paddy soil
SiO_2	37.82	0.87	64.13
Al_2O_3	30.83	0.69	19.50
CaO**	9.44	23.68	0.63
Fe_2O_3*	7.81	0.16	6.10
K_2O**	2.07	nd	2.49
MgO**	1.23	0.14	1.41
P_2O_5**	-	-	0.09
MnO*	0.06	nd	0.13
Na_2O	2.71	0.22	0.10
SO_3**	2.03	64.92	-
TiO_2	0.36	nd	1.07
LOI.	5.41	9.26	4.21

4. The topology of raw materials (bottom ash, FGD gypsum, paddy soil and sawdust) [39]

According to Fig. 4.10a, the scanning electron microscopy (SEM) images show that the largest fraction of BA consisted of hollow spheres. At higher size ranges, porous sponge-like particles were detected. Therefore, it is suggested that bottom ash could be used as nutrient adsorbent. Gypsum in this study is mostly present as massive crystals (Fig. 4.10b). In the FGD process, lime or calcium oxide is injected into the scrubber at low temperature and low oxygen environment. Sulfur, derived from the coal burning process, is not oxidized to sulfate (SO_4^{2-}) due to the limited amount of oxygen available. The sulfur is instead oxidized to sulfite (SO_3^{2-}) and reacts with the lime to form the mineral of calcium sulfate dihydrate or gypsum
($CaSO_4.2H_2O$). The topology of PC shows more layers (Fig 4.10c). PC has high plasticity and CEC. Sawdust consists of long fibers and has highly irregular structure
(see Fig. 4.10a-4.10d). Moreover, after firing, sawdust will be changed to ash leading to high porosity with long pores that allow water and fertilizer solutions pass through the material.

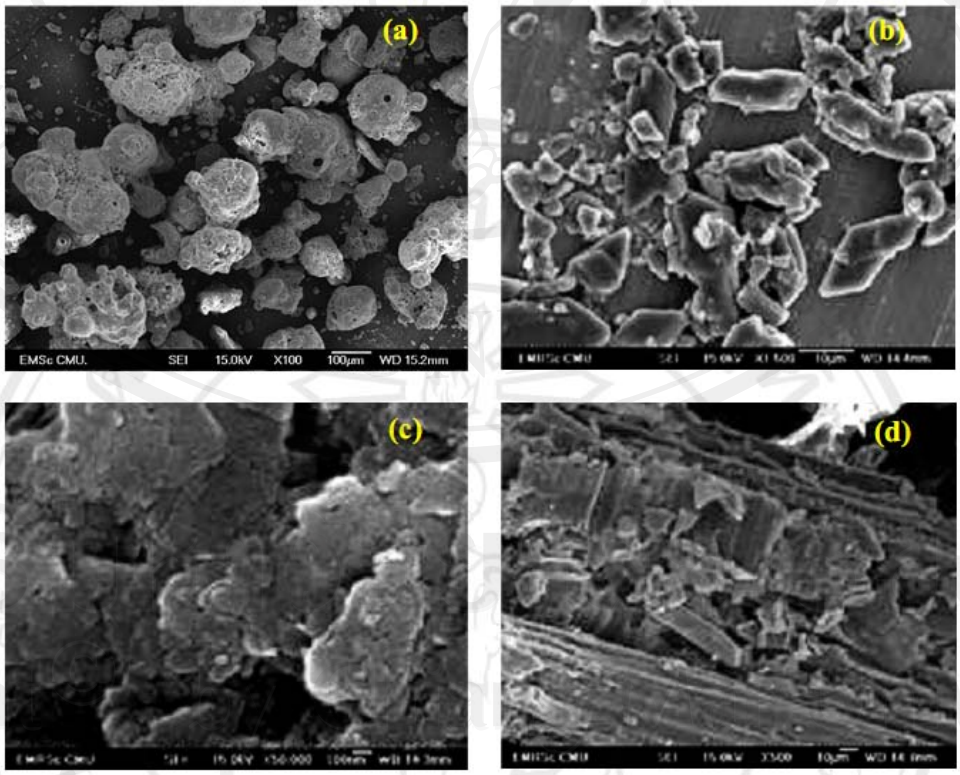

Fig. 4.10 Scanning electron microscopy (SEM) images of raw materials (a) bottom ash, (b) FGD gypsum, (c) paddy soil and (d) sawdust, respectively.

CURRICULUM VITAE

Name Miss Waraporn Sittinang

Date of birth May 5, 1985

Academic status

1) B.S. (Chemistry), Maejo University, 2006

Conferences

1) W. Sittinang, O. Arquero and S. Thiansem and Appropriate composition of preparation of adsorbent material from mixture of bottom ash and FGD gypsum for dye adsorption, Poster presentation, 5-7 january, Congress on Science and Applied Science, Grand Miracle, Bangkok, Thailand, 2011.